

A Dynamic QoS Model for improving the throughput of Wideband Spectrum Sharing in Cognitive Radio Networks

K.Manivannan¹, C.G.Ravichandran² and B.Sakthi Karthi Durai³

¹Department of Computer Science and Engineering,
PSNA College of Engineering & Technology, Dindigul, Tamilnadu-624622, India.

[E-mail: manivannancse@hotmail.com]

²Principal, SCAD Institute of Technology,
Palladam, Tiruppur, Tamilnadu-641664, India.

[E-mail: cg_ravi@yahoo.com]

³Department of Information Technology,
Latha Madhavan Engineering College, Madurai, Tamilnadu, India.

[E-mail: challengersakthi@gmail.com]

*Corresponding author: K.Manivannan

*Received June 18, 2014; revised August 20, 2014; accepted September 10, 2014;
published November 30, 2014*

Abstract

This paper considers a wideband cognitive radio network (WCRN) which can simultaneously sense multiple narrowband channels and thus aggregate the detected available channels for transmission and studies the ergodic throughput of the WCRN that operated under: the wideband sensing-based spectrum sharing (WSSS) scheme and the wideband opportunistic spectrum access (WOSA) scheme. In our analysis, besides the average interference power constraint at PU, the average transmit power constraint of SU is also considered for the two schemes and a novel cognitive radio sensing frame that allows data transmission and spectrum sensing at the same time is utilized, and then the maximization throughput problem is solved by developing a gradient projection method. Finally, numerical simulations are presented to verify the performance of the two proposed schemes.

Keywords: wideband sensing based spectrum sharing, wideband opportunistic spectrum access, cognitive radio networks, Quality of Service.

1. Introduction

With the rapid deployment of various wireless systems, the limited radio spectrum is becoming increasingly crowded. On the other hand, it is evident that most of the allocated spectrum experience low utilization and it is reported by Federal Communications Commission that 70% of the allocated spectrum bands in US are not fully utilized [1]. Cognitive Radio (CR) technology [2][3][21] is considered as a revolutionary paradigm providing high spectrum utilization for wireless communications, in which secondary (unlicensed) users (SUs) who have no spectrum licenses can opportunistically access and share the unused spectrum of primary (licensed) users (PUs) who have spectrum licenses at the premise that the interference from SUs to PUs does not degrade the quality of service (QoS) of PUs. One of the most challenging issues in CR networks [22] is efficient spectrum sharing [4], which allows SU to utilize the licensed spectrum that are not using for PU service. There are in general three strategies proposed for spectrum sharing: The first one is opportunistic spectrum access (OSA) [5], in which the SUs are allowed to access the spectrum that is allocated to PUs when the spectrum is not used by any PU. The second way is spectrum sharing (SS) [6], which allows simultaneous transmission of PUs and SUs. From PU's perspective, SUs are allowed to coexist with PUs as long as the interference from SU does not degrade the QoS [23] of PU to an acceptable level [20]. From SU's perspective, SU should control its transmit power properly in order to achieve a reasonably high transmission rate without causing too much interference to PU. The latter one is sensing-based spectrum sharing (SSS) [7], where SUs sense the status of the channel and adapted their transmit power according to the decisions made by spectrum sensing. If the spectrum is occupied, SUs transmit with low power, and on the other hand if the spectrum is available, SUs transmit with high power. The latter approaches can be seen as a hybrid approach between the first one and the second one. A typical frame structure for the SU is presented in Fig. 1 which comprises of the sensing and data transmission slots. In the sensing slot, the SU senses the status of the PU (active/idle) and in the remaining duration, data transmission is accomplished based on the sensing results made by spectrum sensing. Hence, the sensing-throughput trade off problem exists [7][8][9]. This problem which utilizes energy detection [10] for spectrum sensing was addressed in [8] for a single frequency band, where the authors investigated the problem of finding the optimal sensing time that maximizes the achievable ergodic throughput under a constraint on the interference power at the PU. In [7], the design of the sensing time has been addressed in order to maximize the average achievable throughput under the SU's own transmit-power constraint (which was not considered in [8]). This work was extended in [9] for a wideband spectrum, where the problem of designing the optimal sensing time that maximizes the throughput of WSSS and WOSA schemes for WCRN were studied. Different from [7] and [8] the authors in [9] introduce combined average transmit power and interference power constraints in the schemes, in order to control the transmission powers of the SUs and effectively protect the PU from harmful interference

respectively. However, this typical frame structure decreases the ergodic throughput by a factor of $T - T/T$. In addition, the problem of the optimal sensing time is an issue. Motivated by the previous work, this paper address two schemes, namely

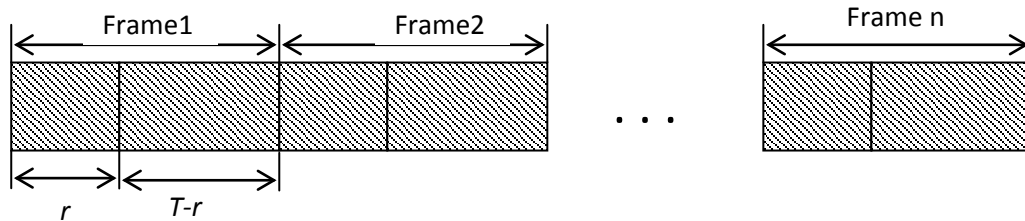


Fig. 1. Typical sensing frame structure

proposed wideband sensing-based spectrum sharing (PWSSS) and proposed wideband opportunistic spectrum access (PWOSA) scheme, in which another frame structure proposed in [11] is unitized that overcomes the sensing-throughput tradeoff in WCRN by allowing spectrum sensing and data transmission at the same time. This new model will be described in Section II in more detail. Moreover, we study the problem of maximizing the achievable ergodic throughput of the proposed two schemes under joint average transmit power and interference power constraints without exceeding the power limit of the SU or causing harmful interference to the PU. It is shown that there is a throughput gain for SU under the average over the peak transmit and interference power constraints [12][13]. Furthermore, we discuss the effect of the average transmit power constraint and the average interference power constraint on the ergodic throughput and simulate the performances of the two schemes. The rest of this paper is organized as follows. Section II presents the system model while Section III and IV investigate the problem of maximizing the ergodic throughput under joint average transmit power and average interference power constraints for the PWSSS scheme and PWOSA scheme respectively. The simulation results are presented and discussed in Section V. Finally, Section VI concludes this paper.

2. System Model

To provide better service for SUs, it is advisable to aggregate the perceived spectrum opportunities obtained through simultaneous sensing over wideband channel. So this paper considers a WCRN where SUs can access a wideband spectrum licensed to a PU under WSSS scheme and WOSA scheme. Assume that the wideband spectrum is divided into M equally spaced orthogonal narrowband channels. In order to access the frequency band, the SUs must first perform spectrum sensing to determine the status (active or idle) of each channel and it can only access the channel when the PU is not present. The wideband joint detector propose in [14] is utilized in this paper, in which the energy detector is adopted to sense spectrum opportunities on each channel simultaneously. **Fig.**

2 shows the system model of wideband spectrum sensing. The noise at the SUs is assumed to be circularly symmetric complex Gaussian (CSCG) with zero mean and σ^2n variance, namely CN $(0, \sigma^2n)$. The instantaneous channel power gains from the SU's transmitter (SU-Tx) to the SU's receiver (SU-Rx) and the PU's receiver (PU-Rx) for the channel and PU's transmitter (PU-Tx) to the SU-Rx are denoted by $g_{ss,i}$, $g_{sp,i}$, $g_{ps,i}$ respectively, and the channels are assumed to be flat fading and the channel power gains to be ergodic, stationary and know at the SUs similar to [7][10][15]. The received signal at the SU-Rx on channel i is given by

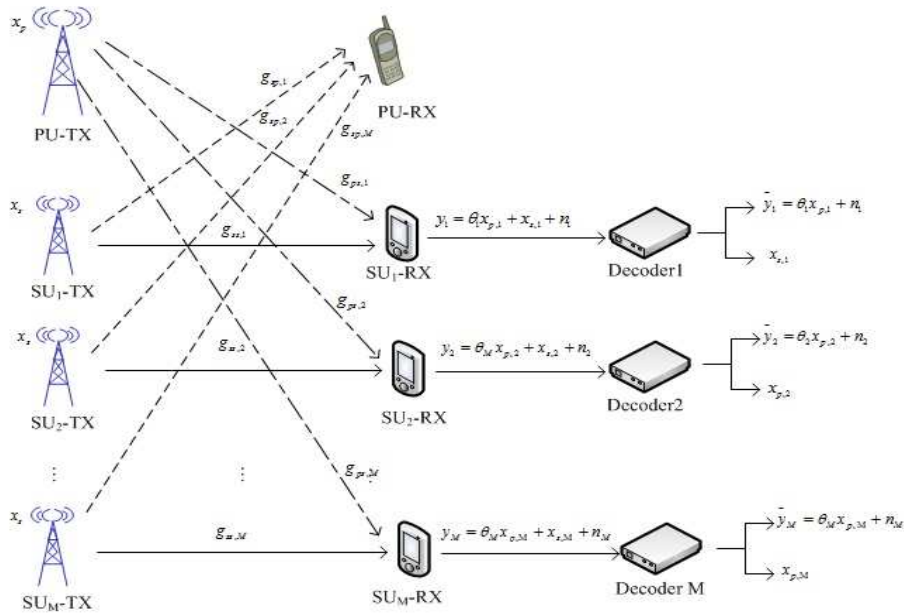


Fig. 2. System model of wideband spectrum sharing

$$y_i = \theta_i x_{p,i} + x_{s,i} + n_i \tag{1}$$

where Θ_i denotes the actual status of the i -th narrowband, $\Theta_i= 1$ denotes that there is PU transmitting on the i -th narrowband, while $\Theta_i= 0$ denotes that there is no PU on the i -th narrowband, $x_{p,i}$, $x_{s,i}$ represent the received signal for the PU and the received signal for the SU on the i -th narrowband channel respectively. Finally n_i is the additive noise on channel i . Consider a similar scenario to spectrum sharing CRN [6] [12], where the SUs are able to decode the received secondary signal irrespective of the status of the PU. The received signal on channel i is initially passed through the decoder as depicted in Fig. 2, where the signal from the SU's transmitter (SU-Tx) is obtained [6] [12]. In the following,

the signal from SU-Tx is cancelled out from the aggregate received signal y_i and the remaining signal

$$y_i^{\wedge} = \theta_i x_{p,i} + n_i y_i \quad (2)$$

is used to sense the spectrum on channel i . The detection and false alarm probabilities for the i -th channel are given by

$$P_{d,i} = Q\left(\left(\frac{\eta_i}{\sigma_n^2} - \gamma_i - 1\right) \sqrt{\frac{\tau f_s}{2\gamma_i + 1}}\right) \quad (3)$$

$$P_{fa,i} = \left(\sqrt{2\gamma_i + 1} Q^{-1}(P_{d,i}) + \sqrt{\tau f_s \gamma_i}\right) \quad (4)$$

respectively [5], where τ denotes the sensing time, η_i is the decision threshold of the energy detector on channel i , γ_i represents the received signal to noise ratio (SNR) from the PU at the secondary detector on channel i and f_s is the sampling frequency.

2.1. New Sensing Frame Structure

Fig. 3 shows the new sensing frame structure proposed in [11] under the system in **Fig. 2**. It can be easily obtained from the **Fig. 3** that SUs are able to sense the spectrum and transmit the data at the same time almost during the whole duration of the new sensing frame. Compared with the frame shown in **Fig. 1**, the new frame is able to maximize both the sensing and transmitting time for SUs, thus improving the sensing throughput of SUs. The obvious significances of the new frame structure are as follows.

- Almost the whole duration of the new frame structure can be utilized to sense the spectrum and transmit the data at the same time for SUs.
- The new frame increases the sensing time, thus more complex spectrum detection schemes which require higher sensing time can be utilized to sense the presence of PU to provide higher sensing accuracy.
- The new frame increases the throughput of CRN because the sensing time slot in **Fig. 1** is now used for data transmission and the problem of optimal sensing time is no longer an issue.
- This new frame structure facilitates continuous transmission of the SU.

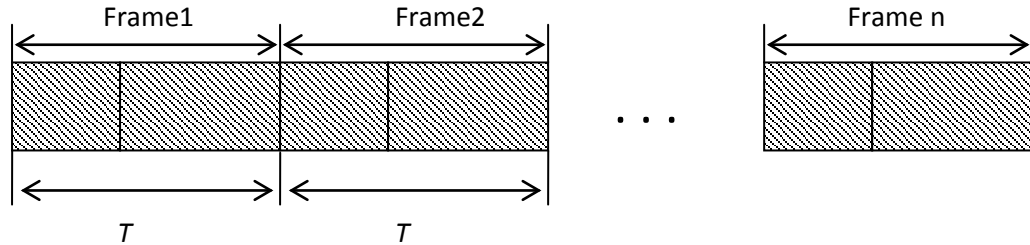


Fig. 3. New sensing frame structure

3. Proposed Scheme

In the PWSSS scheme which utilizes the new sensing frame in Fig. 3, the SUs simultaneously sense and access to M narrowband and adapt their transmit power on each channel based on the sensing

results obtained by spectrum sensing. If the PU on the i -th channel is detected to be absent, the SUs transmit with high power $P_{s,i}^{(0)}$ on the i -th channel in order to transmit more data for themselves and on the opposite side if the PU is detected to be present, the SUs transmit with a low power $P_{s,i}^{(1)}$ on the i -th channel in order to control the interference level to the legal PU. In general speaking, $P_{s,i}^{(0)} > P_{s,i}^{(1)}$. Moreover, assume that the PU transmits with power $P_{p,i}$ on the i -th channel. Therefore, based on the sensing results (absent/present) and the actual status (idle/active) of the PU, there are four instantaneous transmission rates distinguished for the i -th narrowband: $r_{00,i} = \log_2(1 + g_{ss,i} P_{s,i}^{(0)} / \sigma_n^2)$, $r_{01,i} = \log_2(1 + g_{ss,i} P_{s,i}^{(1)} / \sigma_n^2)$, $r_{10,i} = \log_2(1 + g_{ss,i} P_{s,i}^{(0)} / (g_{ps,i} P_{p,i} + \sigma_n^2))$, $r_{11,i} = \log_2(1 + g_{ss,i} P_{s,i}^{(1)} / (g_{ps,i} P_{p,i} + \sigma_n^2))$. Here, the first index number of the instantaneous transmission rates denotes that the actual status of the PU ("0" for idle, "1" for active) and the second index number indicates the sensing results detected by SU ("0" for absent, "1" for present), finally the third index number indicates the i -th narrowband. In real-time environment, spectrum sensing is always imperfect and the sensing errors may happen due to missed and false detection of the spectrum. Table 1 lists four possible scenarios under the transmission model in real-time environment according to the actual status of the PU and the decisions made by SUs. It can be clearly obtained from Table 1 that when the spectrum is actually occupied by the PU and wrongly considered idle, the SU still transmits with high power $P_{s,i}^{(0)}$ because it is not aware of the presence of the PU. On the other hand, when a false alarm happens, the SU still transmits with low power $P_{s,i}^{(1)}$ even if the channel is available to SU. Therefore, the total ergodic throughput of the i -th channel for the PWSSS scheme is given by

$$C_i = a_{0,i} r_{00,i} + a_{1,i} r_{01,i} + b_{0,i} r_{10,i} + b_{1,i} r_{11,i} \tag{5}$$

Table 1. Possible transmit power and rate.

PU's actual status	Sensing results	Related Probability	Transmit power	Transmit rate
1	1	$P_{d,i}$	$P_{s,i}^{(1)}$	$r_{11,i}$
1	0	$1 - P_{d,i}$	$P_{s,i}^{(0)}$	$r_{10,i}$
0	1	$P_{fa,i}$	$P_{s,i}^{(1)}$	$r_{01,i}$
0	0	$1 - P_{fa,i}$	$P_{s,i}^{(0)}$	$r_{00,i}$

where $a_{0,i} = P(H_{0,i})(1 - P_{fa,i})$, $b_{0,i} = P(H_{1,i})(1 - P_{d,i})$, $a_{1,i} = P(H_{0,i})P_{fa,i}$, $b_{1,i} = P(H_{1,i})P_{d,i}$, $P(H_{0,i})$ and $P(H_{1,i})$ represent the idle and active probability of the i -th channel respectively. In the PWSSS, due to the coexistence with PU, the harmful interference at the PU-Rx should not exceed the given threshold. At the same time, in order to control the transmit power of SU, the transmit power of SU should under a predefined threshold. SU's average transmit power and interference power at PU constraints which can be written as

$$E\left\{\sum_{i=1}^M [a_{0,i}P_{s,i}^{(0)} + a_{1,i}P_{s,i}^{(1)} + b_{0,i}P_{s,i}^{(0)} + b_{1,i}P_{s,i}^{(1)}]\right\} \leq P_{av} \quad (6)$$

$$E\{b_{0,i}g_{sp,i}P_{s,i}^{(0)} + b_{1,i}g_{sp,i}P_{s,i}^{(1)}\} \leq \Gamma, i = 1, \dots, M \quad (7)$$

where P_{av} denotes the predefined threshold of average transmit power of the SUs, and Γ represents the predefined threshold of average interference power that is tolerable by PU. Therefore, the maximizes ergodic throughput of the PWSSS under the new sensing frame can be obtained by solving the following optimization problem

$$P : \{P_{s,i}^{(0)}, P_{s,i}^{(1)}\} R\{P_{s,i}^{(0)}, P_{s,i}^{(1)}\} = \sum_{i=1}^M C_i \quad (8)$$

Based on the Lagrangian method [16], the problem (8) is equivalent to find the minimum of Lagrangian function:

$$\begin{aligned} & L(P_{s,i}^{(0)}, P_{s,i}^{(1)}, \lambda, \mu_i) \\ &= E\left\{\sum_{i=1}^M (a_{0,i}r_{00,i} + a_{1,i}r_{01,i} + b_{0,i}r_{10,i} + b_{1,i}r_{11,i})\right\} \\ & - \lambda [E\left\{\sum_{i=1}^M [a_{0,i}P_{s,i}^{(0)} + a_{1,i}P_{s,i}^{(1)} + b_{0,i}P_{s,i}^{(0)} + b_{1,i}P_{s,i}^{(1)}]\right\} - P_{av}] \\ & - \sum_{i=1}^M \mu_i [E\{b_{0,i}g_{sp,i}P_{s,i}^{(0)} + b_{1,i}g_{sp,i}P_{s,i}^{(1)}\} - \Gamma] \end{aligned} \quad (9)$$

where λ, μ_i are non-negative Lagrangian multipliers associated with the transmit power

constraint of SU and interference constraint at PU and the dual function is given by

$$g(\lambda, \mu_i) = \min_{P_{s,i}^{(0)}, P_{s,i}^{(1)}} L(P_{s,i}^{(0)}, P_{s,i}^{(1)}, X, \mu_i) \quad (10)$$

In order to calculate the dual function $g(\lambda, \mu_i)$, the supremum of the Lagrangian with respect to $P_{s,i}^{(0)}$ and $P_{s,i}^{(1)}$ need to be found. This problem can be decomposed into two sub-dual-problems:

$$\begin{aligned} \maximize \quad & E\left\{\sum_{i=1}^M a_{0,i} r_{00,i} + b_{0,i} r_{10,i}\right\} \\ P_{s,i}^{(0)} \geq 0 \quad & -\lambda E\sum_{i=1}^M [a_{0,i} P_{s,i}^{(0)} + b_{0,i} P_{s,i}^{(0)}] \\ & -\sum_{i=1}^M \mu_i [E\{b_{0,i} g_{sp,i} P_{s,i}^{(0)}\}] \end{aligned} \quad (11)$$

$$\begin{aligned} \maximize \quad & E\left\{\sum_{i=1}^M a_{1,i} r_{11,i} + b_{1,i} r_{01,i}\right\} \\ P_{s,i}^{(1)} \geq 0 \quad & -\lambda E\sum_{i=1}^M [a_{1,i} P_{s,i}^{(1)} + b_{1,i} P_{s,i}^{(1)}] \\ & -\sum_{i=1}^M \mu_i [E\{a_{1,i} g_{sp,i} P_{s,i}^{(1)}\}] \end{aligned} \quad (12)$$

One for each transmit power. These two problems are convex optimization problems, Karush-KuhnTucker (KKT) conditions are applied to find the optimum solution. The optimal power allocation is obtained as [17]

$$P_{s,i}^{(0)} = \left[\frac{A_{0,i} + \Delta_{0,i}}{2} \right]_+, P_{s,i}^{(1)} = \left[\frac{A_{1,i} + \Delta_{1,i}}{2} \right]_+ \quad (13)$$

$$A_{0,i} = \frac{\log_2(e)(a_{0,i} + b_{0,i})}{\lambda(a_{0,i} + b_{0,i}) + \mu_i b_{0,i}, g_{sp,i}} - \frac{2\sigma_n^2 + g_{sp,i} P_{p,i}}{g_{ss,i}} \quad (14)$$

$$\Delta_{0,i} = A_{0,i}^2 - \frac{4}{g_{ss,i}} \left\{ \frac{\sigma_n^2 + g_{ps,i} P_{p,i}}{g_{ss,i} \sigma_n^{-2}} - \frac{\log_2(e)(a_{0,i}(2\sigma_n^2 + g_{sp,i} P_{p,i}) + b_{0,i} \sigma_n^2)}{\lambda(a_{0,i} + b_{0,i}) + \mu_i b_{0,i}, g_{sp,i}} \right\} \quad (15)$$

$$A_{1,i} = \frac{\log_2(e)(a_{1,i} + b_{1,i})}{\lambda(a_{1,i} + b_{0,i}) + \mu_i b_{1,i}, g_{sp,i}} - \frac{2\sigma_n^2 + g_{sp,i} P_{p,i}}{g_{ss,i}} \tag{16}$$

$$\Delta_{1,i} = A_{1,i}^2 - \frac{4}{g_{ss,i}} \left\{ \frac{\sigma_n^2 + g_{ps,i} P_{p,i}}{g_{ss,i} \sigma_n^{-2}} - \frac{\log_2(e)(a_{1,i}(2\sigma_n^2 + g_{sp,i} P_{p,i}) + b_{1,i} \sigma_n^2)}{\lambda(a_{1,i} + b_{1,i}) + \mu_i b_{1,i}, g_{sp,i}} \right\} \tag{17}$$

and $[x]^+$ denotes $\max(x, 0)$. In order to solve the problem in (8), i.e., to find the optimal values for multipliers λ and μ_i . We apply the gradient projection method [18], which requires the calculation of the subgradient of λ and μ_i . Since the subgradients of λ and μ_i are given by $(P_{av} - E\{\sum_{i=1}^M [(a_{0,i} + b_{0,i})P_{s,i} + (a_{1,i} + b_{1,i})P_{s,i}]\})$ and $(\Gamma - E\{g_{sp,i} b_{0,i} P_{s,i} + g_{sp,i} b_{1,i} P_{s,i}\})$, respectively, where $i = 1, \dots, M$. λ and μ_i can be obtained from

$$\lambda_{k+1} = [\lambda_k + \alpha \{ E\{ \sum_{i=1}^M [(a_{0,i} + b_{0,i})P_{s,ik}^{(0)}] + (a_{1,i} + b_{1,i})P_{s,ik}^{(1)} \} - P_{av}]^+ \tag{18}$$

$$\mu_{i,k+1} = [\mu_{i,k} + \alpha \{ E\{ g_{sp,i} b_{0,i} P_{s,k}^{(0)} + g_{sp,i} b_{1,i} P_{s,k}^{(1)} \} - \Gamma]^+ \tag{19}$$

where α is the step size. From literature [19], we can obtain that if the step size α is small enough, the dual variables can converge to the optimal value λ^*, μ_i^* within a small area. Under this, $P_{s,i}^{(0)*}$ and $P_{s,i}^{(1)*}$ can be obtained through substituting (14)-(17) in to (13).

Proof: See Appendix.

The steps of the PWSSS algorithm that utilizes the gradient projection method [18] are as follows.

Step1: Initialize $\lambda_1, \mu_i, 1, k = 1$;

Step2: Calculate $P_{s,ik}$ and $P_{s,ik}$ using equation (13)-(17);

Step3: Calculate the search direction:

$$d_{\lambda_k} = [E\{\sum_{i=1}^M [(a_{0,i} + b_{0,i})P_{s,ik}^{(0)}] + (a_{1,i} + b_{1,i})P_{s,ik}^{(1)}\} - P_{av}]^+,$$

$$d_{\mu_k} = [E\{g_{sp,i}b_{0,i}P_{s,k}^{(0)} + g_{sp,i}b_{1,i}P_{s,k}^{(1)}\} - \Gamma]^+;$$

Step4: If $d_{\lambda_k} < \varepsilon$, $d_{\mu_k} < \varepsilon$, $(P_{s,i,k}, P_{s,i,k}) = (P_{s,i,k}, P_{s,i,k})$ is the approximate optimal solution, else update by (18),(19);

Step5: $k = k + 1$, go to step 3.

4.1. Proposed Wideband Opportunistic Spectrum Access Scheme

In the PWOSA scheme which also utilizes the novel sensing frame in Fig. 3, the SUs simultaneously sense all the narrow bands and can access to the spectrum bands only when noise are detected to be available. However, as mentioned in the section III, due to the limitations of spectrum sensing techniques and the nature of wireless communications in real-time environment, spectrum sensing is always imperfect and the sensing errors may happen due to missed and false detection of the spectrum. Missed detection leads to more collisions between the SUs and the PU where the channel is wrongly considered idle, whereas the false alarm makes the SU keep silent even if the idle channel is available to SU. In the PWOSA scheme, we consider the average transmit power constraint given by equation (6) as well as average interference power constraint obtained by equation (7) like the PWSSS scheme. So the optimization problem that maximized the ergodic throughput of the proposed OSA scheme can be formulated as follows

$$\begin{aligned} & \max_{\{P_{s,i}^{(0)}, P_{s,ik}^{(1)}\}} \text{imize} && R(P_{s,i}^{(0)}, P_{s,ik}^{(1)}) = E\{\sum_{i=1}^M C_i\} \\ & \text{subject to} && (6), (7), P_{s,i}^{(0)} \geq 0, P_{s,i}^{(1)} = 0 \end{aligned} \quad (20)$$

It can be seen from (20) that the PWOSA scheme has the same form as the PWSSS problem (8) for $P_{s,i}^{(1)} = 0$. This is no surprise, since the difference between the two schemes is that in the PWOSA scheme, a SU is not allowed to access the spectrum that is utilized by PU while in the PWSSS scheme, a SU is allowed to coexist with the PU and transmit with power $P_{s,i}^{(1)}$ when the spectrum is active. As a result, PWSSS algorithm can be used to solve the maximization ergodic throughput problem for the PWOSA scheme by setting $P_{s,i}^{(1)} = 0$.

5. Simulation Results

In this section, numerical simulations were presented to compare the performance of the conventional wideband sensing based spectrum sharing (CWSSS) utilized typical sensing frame and PWSSS scheme utilized new sensing frame. In addition, the comparisons of PWSSS scheme and PWOSA scheme are also discussed. The parameter settings are shown in [Table 2](#).

Table 2. Parameter settings.

Sensing Time T	95ms
Sampling frequency f_s	7MHZ
The probability that PU is idle $P(H_0)$	{ 0.6, 0.7, 0.8, 0.9 }
The detection probability P_d	0.94
Maximum average transmit power P_{av}	{ 0 ~ 25 } dB
Maximum average interference power Γ	{ -25 ~ -5 } dB
SNR γ	{ -20, -20, -15, -12 } dB
The noise σ_n^2	2
Number of narrowband channels M	4

5.1. Comparison of PWSSS and CWSSS schemes

In [Fig. 4](#), the ergodic throughput versus the sensing time τ is presented for the PWSSS scheme and the CWSSS scheme that employs the conventional frame structure in [Fig. 1](#) for different values of the average transmit power P_{av} of the SUs. The threshold of the average interference power tolerated by PU is set to $\Gamma = 10$ dB, whereas the probability that the frequency band i is idle is assumed to be $P(H_{0,i}) = 0.7$, $i = 1, 2, 3$. It can clearly obtain that the ergodic throughput of the PWSSS is significantly higher compared to the CWSSS. This phenomenon can be explained by the fact that the whole duration of the frame T is used for data transmission in the PWSSS, as opposed to the CWSSS, where only a part of the frame is used for data transmission. Moreover, the ergodic throughput for $P_{av} = 15$ dB is much larger than that for $P_{av} = 10$ dB and $P_{av} = 5$ dB both in PWSSS and CWSSS scheme. This indicates that the SU's transmit power constraint has great influence on the ergodic throughput.

[Fig. 5\(a\)](#) and [Fig. 5\(b\)](#) show the ergodic throughput versus average transmit power P_{av} of the SUs for the PWSSS and the CWSSS, for different $P(H_0)$ under the same maximum average interference power Γ . It is clear that the ergodic throughputs of PWSSS and CWSSS schemes increase with the increase in $P(H_0)$. This is reasonable due to the fact that a larger $P(H_0)$ indicates a higher probability that the licensed channel is available and there will be more chance for SU to transmit their data with higher transmit power. In addition, it is evident from [Fig. 5\(a\)](#) and [Fig. 5\(b\)](#) that the ergodic throughput of the

PWSSS is always larger than those of the CWSSS. This shows the superiority of the novel sensing frame structure which is utilized in the PWSSS scheme. In **Fig. 6(a)** and **Fig. 6(b)**, the ergodic throughput versus the transmit power P_{av} of the SUs for the PWSSS algorithm and CWSSS are presented for various values of the interference power Γ at PU and for $P(H_{0,i}) = 0.7, j = 1, 2, 3$. It can be clearly obtain from **Fig. 6(a)** and **Fig. 6(b)** that the ergodic throughputs of the PWSSS scheme are always larger than those of the CWSSS scheme. This shows the superiority of the novel sensing frame structure which is utilized in the PWSSS scheme. In addition, it is seen from the figure that the ergodic throughput increase with the increase in both the transmit power constraint and the interference power constraint. In addition, it can be obtained from **Fig. 6(a)** and **Fig. 6(b)** that the ergodic throughput doesn't increase when the average transmit power arrives at a fixed value. In this case, the interference power at PU becomes the main constraint

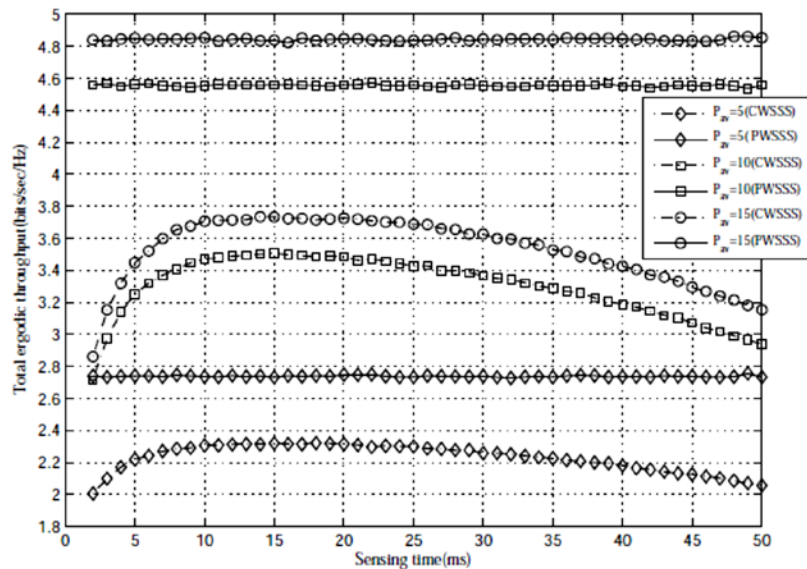


Fig. 4. Ergodic throughput of the PWSSS and CWSSS schemes versus the sensing time τ .

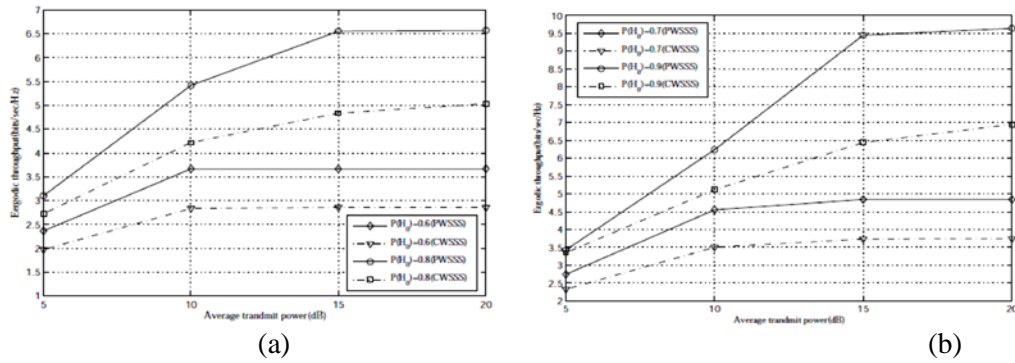


Fig. 5. Ergodic throughput versus total transmit power P_{av} for different values of $P(H_{0,i})$ under $\Gamma = -10$ dB.

5.2. Comparison of PWSSS and PWOSA schemes

Fig. 7(a) and **Fig. 7(b)** show the ergodic throughput versus average transmit power P_{av} of the SUs for PWSSS and the PWOSA, for different $P(H_0)$ under the same maximize average interference power Γ . It is clear that the ergodic throughput of PWSSS scheme and PWOSA scheme increase with the increase in $P(H_0)$. This is reasonable due to the fact that a larger $P(H_0)$ indicates a higher probability that the PU is absence and there will be more chance for SU to transmit their data with a higher power. In addition, it is evident from **Fig. 7(a)** and **Fig. 7(b)** that the ergodic throughput of PWSSS is always larger than those of PWOSA. This shows the superiority of the sensing-based spectrum sharing model adopted in PWSSS scheme.

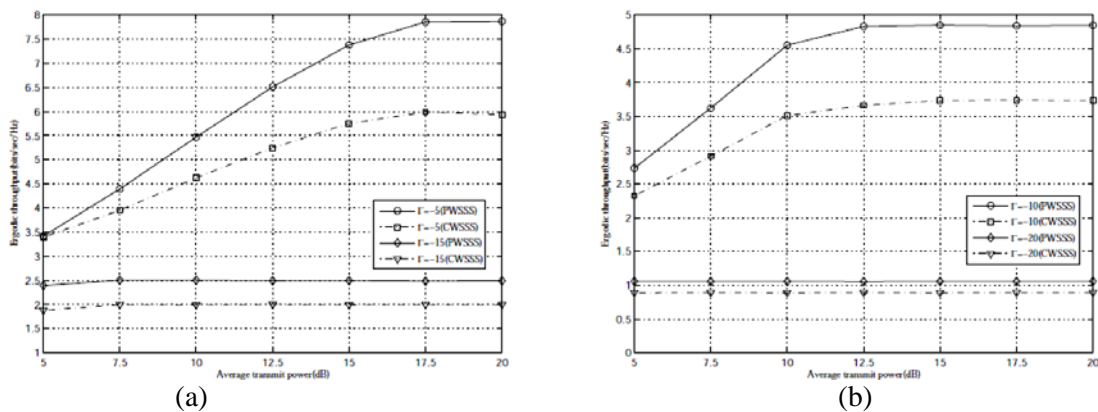


Fig. 6. Ergodic throughput versus transmit power P_{av} for different values of Γ under $P(H_{0,i}) = 0.7, i = 1, 2, 3$.

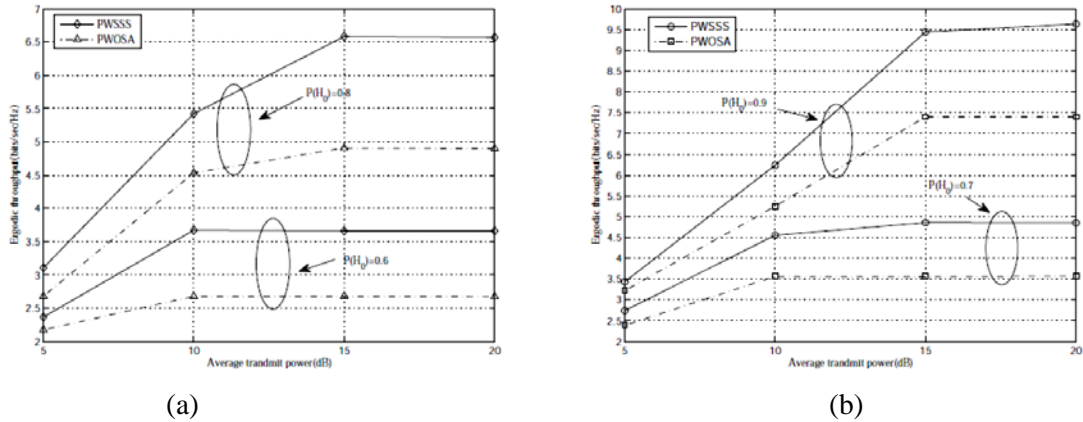


Fig. 7. Ergodic throughput versus transmit power P_{av} for different values of Γ under $P(H_{0,i}) = 0.7, i = 1, 2, 3$.

In **Fig. 8**, the ergodic throughput versus the average transmit power P_{av} of the SUs for the PWSSS algorithm and PWOSA algorithm are presented for various values of the interference power Γ at PU and for $P(H_{0,i}) = 0.7, j = 1, 2, 3$. It can be clearly obtain from Fig. 8 that the ergodic throughputs of the PWSSS scheme are always larger than those of the PWOSA scheme. This shows the superiority of the sensing-based spectrum model. In addition, it is seen from the figure that the ergodic throughput increase with the increase in both the transmit power constraint and the interference power constraint. Moreover, the smaller the Γ , the smaller the difference between ergodic throughput for PWSSS and PWOSA. This can be explained by the fact that the SU's transmit power in the PWSSS is mainly allocated at the periods when the spectrum is available, and the contribution of the PWSSS is significant only when the interference power Γ receives higher values. In addition, the ergodic throughput for $\Gamma = -5$ dB is much larger than that for $\Gamma = -10$ dB and $\Gamma = -15$ dB both in PWSSS and PWOSA scheme. This indicates that the interference constraint Γ has great influence on the ergodic throughput. In addition, it can be obtained from Fig. 8 that the ergodic throughput doesn't increase when the average transmit power arrives at a fixed value. In this case, the interference power at PU becomes the main constraint.

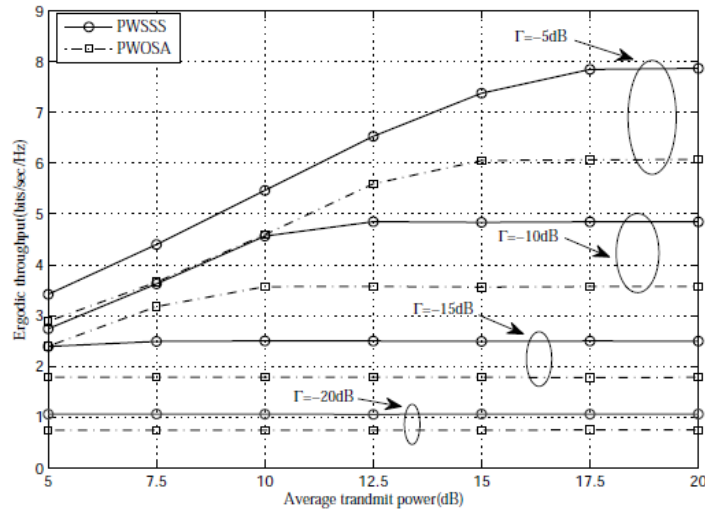


Fig. 8. Ergodic throughput versus transmit power P_{av} for different interference power Γ under $P(H_{0,i}) = 0.7, i = 1, 2, 3$.

In **Fig. 9**, the ergodic throughput versus the interference power Γ at the PU for the PWSSS algorithm and PWOSA algorithm are presented for various values of the average transmit power P_{av} of SUs and for $P(H_{0,i}) = 0.7, i = 1, 2, 3$. It can be clearly obtain from **Fig. 9** that the ergodic throughputs of the PWSSS scheme are always larger than those of the PWOSA scheme. This shows the superiority of the sensing-based spectrum model. In addition, the ergodic throughput for $P_{av} = 15\text{dB}$ is much larger than that for $P_{av} = 5\text{ dB}$ and $P_{av} = 0\text{ dB}$ both in PWSSS and PWOSA scheme. This indicates that the transmit power constraint P_{av} of the SUs has great influence on the ergodic throughput. Moreover, it can be obtained from Fig. 9 that the ergodic throughput doesn't increase when the average interference power arrives at a fixed value. In this case, the transmit power of SUs becomes the main constraint. In **Fig. 10**, the ergodic throughput of the PWSSS and PWOSA scheme are presented versus the additional channel power gain attenuation between the SU-Tx and PU-Rx under $\Gamma = -10\text{ dB}$ and $P_{av} = 15\text{ dB}$. Note that, with increasing channel attenuation, it is observed that the total ergodic throughput increases for both PWSSS and PWOSA schemes. This is obvious since given the fixed average interference power threshold at the PU, increasing the channel attenuation results in increasing of SU's own transmit power.

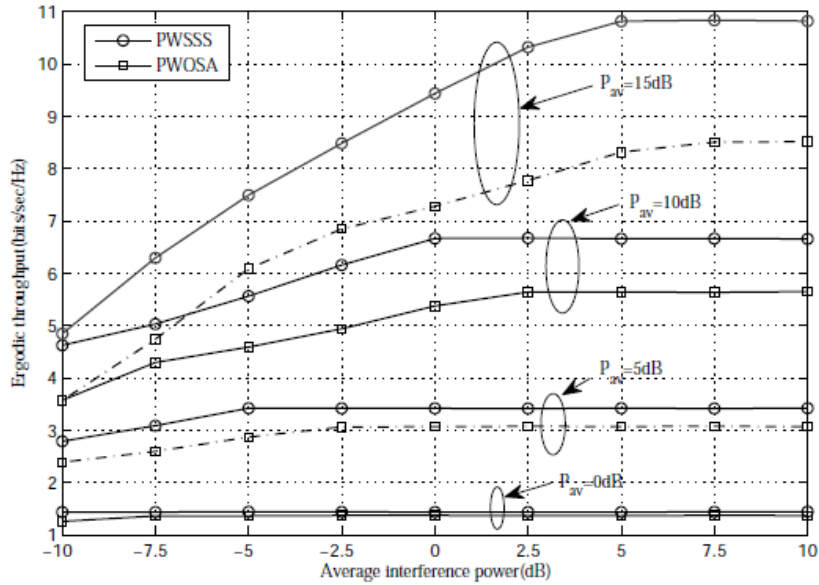


Fig. 9. Ergodic throughput versus interference power Γ for different values of transmit power P_{av} under $P(H_{0,i}) = 0.7$, $i = 1, 2, 3$.

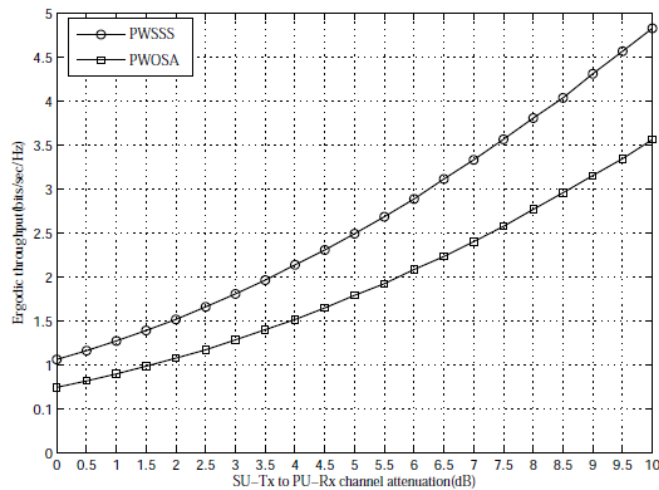


Fig. 10. Ergodic throughput of the PWSS and PWOSA schemes versus the additional channel power gain attenuation.

6. Conclusion

This paper studies the problem of designing the optimal power allocation strategy that maximize the ergodic throughput of PWSSS and PWOSA schemes in cognitive radio networks, subject to different combinations of average transmit and average interference power constraints, which utilize a new sensing frame that significantly improves the throughput by performing data transmission and spectrum sensing at the same time. Simulation results indicate that the PWSSS scheme obtains higher ergodic throughput compared to the PWOSA scheme and CWSSS scheme. Finally, in our future research we plan to extend this work for multiple primary users in CR networks.

Appendix

$$\begin{aligned}
g(\tilde{\lambda}, \tilde{\mu}) &= \min_{\mathbf{P}_s^{(0)}, \mathbf{P}_s^{(1)}} L(\mathbf{P}_s^{(0)}, \mathbf{P}_s^{(1)}, \tilde{\lambda}, \tilde{\mu}) \\
&= E \left\{ \sum_{i=1}^M (a_{0,i} r_{00,i} + a_{1,i} r_{11,i} + b_{1,i} r_{01,i} + b_{0,i} r_{10,i}) \right\} - \\
&\tilde{\lambda} \left\{ E \left\{ \sum_{i=1}^M \left[a_{0,i} P_{s,i}^{(0)} + b_{0,i} P_{s,i}^{(0)} + b_{0,i} P_{s,i}^{(1)} + b_{1,i} P_{s,i}^{(1)} \right] \right\} - P_{av} \right\} \\
&- \sum_{i=1}^M \tilde{\mu}_i \left\{ E \left\{ g_{sp,i} b_{0,i} P_{s,i}^{(0)} + g_{sp,i} b_{1,i} P_{s,i}^{(1)} \right\} - \Gamma \right\} \\
&\geq E \left\{ \sum_{i=1}^M (a_{0,i} \hat{r}_{00,i} + a_{1,i} \hat{r}_{11,i} + b_{1,i} \hat{r}_{11,i} + b_{0,i} \hat{r}_{10,i}) \right\} - \\
&\hat{\lambda} \left\{ E \left\{ \sum_{i=1}^M \left[a_{0,i} P_{s,i}^{(0)} + b_{0,i} P_{s,i}^{(0)} + b_{0,i} P_{s,i}^{(1)} + b_{1,i} P_{s,i}^{(1)} \right] \right\} - P_{av} \right\} \\
&- \sum_{i=1}^M \hat{\mu}_i \left\{ E \left\{ g_{sp,i} b_{0,i} P_{s,i}^{(0)} + g_{sp,i} b_{1,i} P_{s,i}^{(1)} \right\} - \Gamma \right\} \\
&= g(\hat{\lambda}, \hat{\mu}) + (\tilde{\lambda} - \hat{\lambda}) \left(P_{av} - E \left\{ \sum_{i=1}^M \left[a_{0,i} P_{s,i}^{(0)} + b_{0,i} P_{s,i}^{(0)} + b_{0,i} P_{s,i}^{(1)} + b_{1,i} P_{s,i}^{(1)} \right] \right\} \right) \\
&+ \sum_{i=1}^M (\tilde{\mu}_i - \hat{\mu}_i) \left(\Gamma - E \left\{ g_{sp,i} b_{0,i} P_{s,i}^{(0)} + g_{sp,i} b_{1,i} P_{s,i}^{(1)} \right\} \right)
\end{aligned}$$

so the subgradients of λ and μ_i are given by $(P_{av} - E\{\sum_{i=1}^M [(a_{0,i} + b_{0,i})P_{s,i}^{(0)} + (a_{1,i} + b_{1,i})P_{s,i}^{(1)}]\})$ and $(\Gamma - E\{g_{sp,i}b_{0,i}P_{s,i}^{(0)} + g_{sp,i}b_{1,i}P_{s,i}^{(1)}\})$, respectively.

References

- [1] Federal Communications Commission, *Spectrum policy task force report*, pp. 02-15, 2002.
- [2] J. Mitola III, Jr. G. Q. Maguire, "Cognitive radio: making software radios more personal," *IEEE Personal Communications*, vol. 6, pp. 13-18, 1999. [Article\(CrossRef Link\)](#)
- [3] S. Haykin, "Cognitive radio: brain-empowered wireless communications," *IEEE Journal on Selected Areas in Communications.*, vol. 23, pp. 201-220, 2005. [Article \(CrossRef Link\)](#)
- [4] E. Hossain, D. Niyato, Z. Han, "Dynamic spectrum access and management in cognitive radio networks," *Cambridge University Press*, 2009. [Article\(CrossRef Link\)](#)
- [5] A. T. Hoang, Y. C. Liang, D. Wong, et al, "Opportunistic spectrum access for energy-constrained cognitive radios," *IEEE Transactions on Wireless Communications*, vol. 8, pp. 1206-1211, 2009. [Article \(CrossRef Link\)](#)
- [6] A. Ghasemi, E. S. Sousa, "Fundamental limits of spectrum-sharing in fading environments," *IEEE Transactions on Wireless Communications*, vol. 6, pp. 649-658, 2007. [Article \(CrossRef Link\)](#)
- [7] X. Kang, Y. C. Liang, H. K. Garg, et al, "Sensing-based spectrum sharing in cognitive radio networks," *IEEE Transactions on Vehicular Technology*, vol. 58, pp. 4649-4654, 2009. [Article \(CrossRef Link\)](#)
- [8] K. Hamdi, K. B. Letaief, "Power, sensing time, and throughput tradeoffs in cognitive radio systems: a cross-layer approach," *IEEE Wireless Communications and Networking Conference*, pp. 1-5, 2009.
- [9] S. Stotas, A. Nallanathan, "Optimal sensing time and power allocation in multiband cognitive radio networks," *IEEE Transactions on Communications*, vol. 59, pp. 226-235, 2011. [Article \(CrossRef Link\)](#)
- [10] S. Atapattu, C. Tellambura, H. Jiang, "Energy detection based cooperative spectrum sensing in cognitive radio networks," *IEEE Transactions on Wireless Communications*, vol. 10, pp. 1232-1241, 2011. [Article \(CrossRef Link\)](#)
- [11] S. Stotas, A. Nallanathan, "Enhancing the capacity of spectrum sharing cognitive radio networks," *IEEE Transactions on Vehicular Technology*, vol. 60, pp. 3768-3779, 2011. [Article \(CrossRef Link\)](#)
- [12] R. Zhang, "On peak versus average interference power constraints for protecting primary users in cognitive radio networks," *IEEE Transactions on Wireless Communications.*, vol. 8, pp. 2112-2120, 2009. [Article \(CrossRef Link\)](#)
- [13] R. Zhang, X. Kang, Y. C. Liang, "Protecting primary users in cognitive radio networks: peak or average interference power constraint?," in *Proc. of IEEE International Conference on Communications.* , pp. 1-5, 2009. [Article \(CrossRef Link\)](#)
- [14] P. Paysarvi-Hoseini, N. C. Beaulieu, "Optimal wideband spectrum sensing framework for cognitive radio systems," *IEEE Transactions on signal processing*, vol. 59, pp. 1170-1182, 2011. [Article \(CrossRef Link\)](#)
- [15] L. Zhang, Y. C. Liang, Y. Xin, "Joint beam forming and power allocation for multiple access radio systems in cognitive radio networks," *IEEE Journal on Selected Areas in Communications.*, vol. 26, pp. 38-51, 2008. [Article \(CrossRef Link\)](#)
- [16] "Convex optimization in signal processing and communications," *Cambridge university press*, 2010.

- [17] X. Kang, Y. C. Liang, A. Nallanathan, et al, "Optimal power allocation for fading channels in cognitive radio networks: Ergodic capacity and outage capacity," *IEEE Transactions on Wireless Communications*, vol. 8, pp. 940-950, 2009.
[Article \(CrossRef Link\)](#)
- [18] S. Boyd, N. Parikh, E. Chu, et al, "Distributed optimization and statistical learning via the alternating direction method of multipliers," *Foundations and Trends in Machine Learning.*, vol. 3, pp. 1-12, 2011. [Article \(CrossRef Link\)](#)
- [19] C. J. Lin, "Projected gradient methods for nonnegative matrix factorization," *Neural computation.*, vol. 19, pp.2756-2779, 2007. [Article \(CrossRef Link\)](#)
- [20] Minh Jo, Longzhe Han, Dohoon Kim, and Hoh Peter In, "Selfish Attacks and Detection in Cognitive Ad-hoc Networks," *IEEE Network*, Vol. 27, No. 3, pp. 46-50, June 2013. [Article \(CrossRef Link\)](#)
- [21] Lisheng Fan, Xianfu Lei, et.al, "Outdated Relay Selection in Two-way Relay Network," *IEEE Transactions on Vehicular Technology*, vol. 62, no. 8, pp. 4051-4057, Oct. 2013. [Article \(CrossRef Link\)](#)
- [22] Lisheng Fan, Xianfu Lei, et.al, "Outage Probability Analysis and Power Allocation for Two-way Relay Networks with User Selection and Outdated Channel State Information," *IEEE Communications Letters*, vol. 16, no. 5, pp. 638-641, May 2012.
[Article \(CrossRef Link\)](#)
- [23] Ravichandran CG, Manivannan K, "Dynamic Quality of Service Model for improving performance of Multimedia Real-Time Transmission in Industrial Networks," *PLoS ONE A*, vol.9 no.8: e105885. [Article \(CrossRefLink\)](#)



K. Manivannan received B.E degree in Computer Science and Engineering from the Anna University, Chennai and M.E degree in Computer Science and Engineering from the same University. He is currently working toward the Ph.D degree in Computer Science and Engineering at the Anna University Chennai, India. His current research interests include distributed embedded systems, Cognitive radio, distributed systems and network architecture.



C. G. Ravichandran received B.E degree in Electronics and Communication Engineering from Bharathiyar University in 1988 and M.E degree in Electronics Engineering from Anna University, Chennai in 1991. He received the Ph.D degree in Medical Image Processing from Anna University, Chennai in 2009. Currently he is a Principal of SCAD Institute of Technology, Palladam, Tamilnadu, India. His research interests include image segmentation, medical image processing, network architecture, distributed systems and web services.



B. Sakthi Karthi Durai received B.E degree in Computer Science and Engineering from the Anna University, Chennai and M.Tech degree in Information Technology from the Kalasalingam University. He is currently working as a assistant professor in Latha Madhavan Engineering College, Madurai, Tamilnadu, India. His current research interests include distributed multimedia systems, Cognitive networks, Multimedia content retrieval and network architecture.